

This copy is for your personal, non-commercial use only.

If you wish to distribute this article to others, you can order high-quality copies for your colleagues, clients, or customers by [clicking here](#).

Permission to republish or repurpose articles or portions of articles can be obtained by following the guidelines [here](#).

The following resources related to this article are available online at www.sciencemag.org (this information is current as of January 11, 2010):

Updated information and services, including high-resolution figures, can be found in the online version of this article at:

<http://www.sciencemag.org/cgi/content/full/325/5945/1250>

Supporting Online Material can be found at:

<http://www.sciencemag.org/cgi/content/full/325/5945/1250/DC1>

A list of selected additional articles on the Science Web sites **related to this article** can be found at:

<http://www.sciencemag.org/cgi/content/full/325/5945/1250#related-content>

This article **cites 25 articles**, 12 of which can be accessed for free:

<http://www.sciencemag.org/cgi/content/full/325/5945/1250#otherarticles>

This article has been **cited by** 1 articles hosted by HighWire Press; see:

<http://www.sciencemag.org/cgi/content/full/325/5945/1250#otherarticles>

This article appears in the following **subject collections**:

Cell Biology

http://www.sciencemag.org/cgi/collection/cell_biol

scripts per gene (Pearson's correlation coefficient = 0.049, $P = 0.117$ at 0.001 PT and Pearson's correlation coefficient = 0.105, $P < 0.0001$ at 0.01 PT). This suggests that regulatory complexity correlates with transcript complexity. Single-eQTL SNPs were also found to influence expression of multiple genes. At the 0.001 (and 0.01) PT, over 6% (19%) of eQTL SNPs were associated with the expression of more than one gene (fig. S10).

We used gene ontology (GO) (28) to compare the properties of cell type-specific and cell type-shared genes. We found an overrepresentation of functions linked to signal transducer activity, cell communication, development, behavior, cellular process, enzyme regulator activity, transcription regulator activity, and response to stimulus, which reflect processes likely to sculpt cell type-specific profiles. For eQTLs shared in all cell types, we found an overrepresentation of catalytic activity and transport properties (Fisher's exact test, $P < 0.05$) (table S5).

We have demonstrated that variants affecting gene regulation act predominantly in a cell type-specific manner, and even cell types as closely related as LCLs and T cells share only a minority of cis eQTLs. We estimate that 69 to 80% of regulatory variants are cell-type specific and that regulatory variant complexity correlates with transcript complexity, which implies that there are genotype-specific effects on alternative transcript choice. In

addition, cell type-specific eQTLs have smaller effects and tend to localize at greater distances from the TSS, recapitulating enhancer element distributions. The signal of cell-type specificity was shown to be primarily due to differential use of regulatory elements of genes that are expressed in almost all cell types. As more tissues are interrogated, we expect diminishing returns in discovery of eQTLs, and it is possible that there is a minimum set of informative tissues for the majority of regulatory variants. Our study highlights the need for extensive interrogation of regulatory variation in multiple cell types and tissues to elucidate their differential functional properties.

References and Notes

1. A. S. Dimas *et al.*, *PLoS Genet.* **4**, e1000244 (2008).
2. A. L. Dixon *et al.*, *Nat. Genet.* **39**, 1202 (2007).
3. H. H. Goring *et al.*, *Nat. Genet.* **39**, 1208 (2007).
4. M. Morley *et al.*, *Nature* **430**, 743 (2004).
5. E. E. Schadt *et al.*, *Nature* **422**, 297 (2003).
6. B. E. Stranger *et al.*, *PLoS Genet.* **1**, e78 (2005).
7. B. E. Stranger *et al.*, *Nat. Genet.* **39**, 1217 (2007).
8. M. D. Adams *et al.*, *Nature* **377**, 3 (1995).
9. A. Reymond *et al.*, *Nature* **420**, 582 (2002).
10. A. I. Su *et al.*, *Proc. Natl. Acad. Sci. U.S.A.* **99**, 4465 (2002).
11. V. Emilsson *et al.*, *Nature* **452**, 423 (2008).
12. A. J. Myers *et al.*, *Nat. Genet.* **39**, 1494 (2007).
13. E. E. Schadt *et al.*, *PLoS Biol.* **6**, e107 (2008).
14. D. J. Campbell, S. F. Ziegler, *Nat. Rev. Immunol.* **7**, 305 (2007).
15. C. J. Cotsapas *et al.*, *Mamm. Genome* **17**, 490 (2006).

16. C. Wu *et al.*, *PLoS Genet.* **4**, e1000070 (2008).
17. International HapMap Consortium *et al.*, *Nature* **449**, 851 (2007).
18. B. E. Stranger *et al.*, *Science* **315**, 848 (2007).
19. Materials and methods are available as supporting material on Science Online.
20. E. L. Heinzen *et al.*, *PLoS Biol.* **6**, e1 (2008).
21. J. D. Storey, R. Tibshirani, *Proc. Natl. Acad. Sci. U.S.A.* **100**, 9440 (2003).
22. H. H. Goring, J. D. Terwilliger, J. Blangero, *Am. J. Hum. Genet.* **69**, 1357 (2001).
23. J. P. Ioannidis, *Epidemiology* **19**, 640 (2008).
24. K. E. Lohmueller, C. L. Pearce, M. Pike, E. S. Lander, J. N. Hirschhorn, *Nat. Genet.* **33**, 177 (2003).
25. J. B. Veyrieras *et al.*, *PLoS Genet.* **4**, e1000214 (2008).
26. G. A. McVean *et al.*, *Science* **304**, 581 (2004).
27. E. Birney *et al.*, *Nature* **447**, 799 (2007).
28. M. Ashburner *et al.*, *Nat. Genet.* **25**, 25 (2000).
29. We thank N. Hammond for technical help. We acknowledge financial support from the Wellcome Trust and NIH to E.T.D. and Infectigen Foundation, Swiss National Science Foundation and AnEUploidy EU to S.E.A. Gene expression data are deposited in NCBI's Gene Expression Omnibus under accession number GSE17080.

Supporting Online Material

www.sciencemag.org/cgi/content/full/1174148/DC1
Materials and Methods

Figs. S1 to S10

Tables S1 to S5

References

27 March 2009; accepted 14 July 2009

Published online 30 July 2009;

10.1126/science.1174148

Include this information when citing this paper.

Rab35 Controls Actin Bundling by Recruiting Fascin as an Effector Protein

Jun Zhang,¹ Marko Fonovic,^{2,3} Kaye Suyama,¹ Matthew Bogoy,² Matthew P. Scott^{1*}

Actin filaments are key components of the eukaryotic cytoskeleton that provide mechanical structure and generate forces during cell shape changes, growth, and migration. Actin filaments are dynamically assembled into higher-order structures at specified locations to regulate diverse functions. The Rab family of small guanosine triphosphatases is evolutionarily conserved and mediates intracellular vesicle trafficking. We found that Rab35 regulates the assembly of actin filaments during bristle development in *Drosophila* and filopodia formation in cultured cells. These effects were mediated by the actin-bundling protein fascin, which directly associated with active Rab35. Targeting Rab35 to the outer mitochondrial membrane triggered actin recruitment, demonstrating a role for an intracellular trafficking protein in localized actin assembly.

A dynamic actin network is required for normal cell morphology, cell locomotion, and cytokinesis (1, 2). These processes require polymerization of globular actin monomers into filaments and bundling of the filaments under the control of actin-binding proteins (ABPs). Certain ABPs cross-link filamentous actin (F-actin)

into ordered parallel bundles that maintain the structural integrity of the cell and are structural components of filopodia, stereocilia, and microvilli (2–4). It is unclear how cells initiate the dynamic assembly of actin at the right times and places during development, physiological stresses, injury, and disease.

The importance of F-actin bundling during development is readily apparent during bristle formation in *Drosophila*. Bristles are mechanosensory organs found in genetically controlled locations on the cuticle. Their shapes and growth are dependent on actin bundles (5–7). The largest bristles, macrochaetae, are formed by a “shaft” cell that extrudes a cytoplasmic extension. This extension contains evenly distributed microtubules and F-actin bundles located just beneath the plasma membrane (Fig. 1, F and G). Bristle morphologies reflect the organi-

zation of actin bundles and can be used to study the regulation of actin in vivo.

Rab proteins constitute the largest subset of Ras-family small guanosine triphosphatases (GTPases). Rab proteins control formation, motility, and docking of vesicles in specific trafficking pathways (8, 9) by recruiting specific effector proteins to different membrane compartments. Rab proteins are evolutionarily conserved: Each of the >70 types of mammalian Rab proteins is related to a particular *Drosophila* Rab protein. We tested all 31 *Drosophila* Rab GTPases systematically for their abilities to influence fly development, with the use of dominant negative (DN) mutant proteins produced in specific cell types (10). Rab activities are controlled by a cycle of associations with GTP or guanosine diphosphate (GDP). The DN mutants contained a Thr/Ser → Asn mutation that causes the proteins to bind preferentially to GDP and remain inactive. Overproduced DN proteins presumably tie up interacting proteins such as Rab exchange factors in nonproductive associations.

Only one of the 31 *Drosophila* Rab proteins had a strong effect on the actin cytoskeleton. Flies producing DN Rab35 (Rab35DN) in the peripheral nervous system (driven by *prospero-gal4*) exhibited unique and specific bristle morphology defects not seen with any other Rab DN gene. Rab35DN caused the development of adult bristles that had sharp bends, kinks, and forked ends in the thorax (Fig. 1, A to E) and other body regions including the head (fig. S6B). Bristles from Rab35DN-expressing flies, stained with the actin-binding dye phalloidin at 45 to 47 hours after puparium forma-

¹Departments of Developmental Biology, Genetics, and Bioengineering and Howard Hughes Medical Institute, Stanford University School of Medicine, Stanford, CA 94305, USA.

²Department of Pathology and Department of Microbiology and Immunology, Stanford University School of Medicine, Stanford, CA 94305, USA. ³Department of Biochemistry, Molecular and Structural Biology, Jozef Stefan Institute, Jamova ulica 39, 1000 Ljubljana, Slovenia.

*To whom correspondence should be addressed. E-mail: mscott@stanford.edu

tion, had a wavy, loose, and disconnected actin organization (Fig. 1H and fig. S2B) relative to the wild-type control (Fig. 1G and fig. S2A). Similar phenotypes are observed in mutants deficient for certain ABPs (5–7), which suggests that Rab35 may function as an ABP or through ABP(s). In the thoracic cuticle, production of Rab11DN or Rab5DN, which block Rab proteins that regulate endocytic trafficking, caused extensive defects in membrane growth and bristle distribution; these phenotypes are distinct from the Rab35DN effect (10). *Rab35* was ubiquitously expressed, with transcripts and proteins especially abundant in the developing nervous system (fig. S1, C to H).

To test whether the defective-bristle actin phenotype was due to reduced Rab35 function, we expressed *UAS-Rab35* hairpin RNA interference (RNAi) in flies to reduce *Rab35* mRNA (fig. S1A). The RNAi caused the same phenotypes as did Rab35DN (Fig. 1P), which confirmed that the DN protein was inhibiting the intended target. The bristle phenotype caused by Rab35RNAi was completely rescued upon expression of a mouse wild-type *Rab35* gene (Fig. 1Q). In an otherwise wild-type genetic background, mouse Rab35DN caused the same phenotype as did fly Rab35DN (fig. S4C) in the peripheral nervous system. Thus, at least some functions of Rab35 protein are conserved from flies to mammals, an evolutionary span of ~500 million years.

Expressing wild-type Rab35 (Rab35WT) in cultured cells induced multiple filopodia-like cellular

extensions (Fig. 1J and figs. S3, A, B, C, D, and I, and S4E). No such effects were seen upon expression of Rab35DN (Fig. 1K and figs. S3, E to I, and S4F). Similarly, Rab35 induces peripheral processes in Jurkat T cells (11) and neurite outgrowth in PC12 and N1E-115 cells (12). The effect of extra Rab35 on cultured cells might reflect its role in vivo, allowing shaft cells to sprout protrusions during bristle development. Rab35DN, in contrast, stopped filopodia growth in vitro (Fig. 1K and figs. S3, E to H, and S4F) and caused defects in growing bristles in vivo (Fig. 1, B, D, and E). Ubiquitous Rab35DN expression driven by tubulin-gal4 caused lethality in embryos and, over a period of days, the death of cultured cells.

Treating *Drosophila* S2 cells with the actin polymerization inhibitor latrunculin A, but not with the microtubule-disrupting agent nocodazole, efficiently blocked the Rab35-driven morphology change (Fig. 1, L to N). Thus, Rab35 appeared to regulate actin assembly.

To explore how Rab35 influences the actin cytoskeleton, we set out to identify effector proteins that bind Rab35 directly. Rab effectors bind specific Rab proteins; binding is dependent on the Rab protein being in its GTP-bound, active state. The effectors have diverse functions in vesicle sorting, motor protein binding, vesicle trafficking, membrane fusion (13), and other roles yet to be defined. We used affinity chromatography to purify proteins that preferentially bind Rab35-GTP, which has been used to identify

other Rab effectors (14). Purified glutathione S-transferase (GST)-tagged Rab35WT protein was loaded with guanosine 5'-O-(3'-thiotriphosphate) (GTP- γ -S) or with GDP and incubated with bovine brain cytosolic extracts. Several proteins were found to bind Rab35-GTP- γ -S specifically (fig. S5A and table S1). Mass spectrometry revealed a prominent 55-kD polypeptide that bound Rab35-GTP- γ -S to be fascin. Myc-tagged Rab35 and FLAG-tagged fascin coimmunoprecipitated from cell extracts. Fascin bound more strongly to Rab35WT than to Rab35DN (Fig. 2A). Purified GST-Rab35 fusion protein bound fascin in vitro (Fig. 2B). Thus, Rab35 binds fascin directly. Fascin bound more strongly to Rab35WT preloaded with GTP- γ -S than to Rab35WT preloaded with GDP in immunoprecipitations of endogenous Rab35 from fly cells and in GST pull-downs (fig. S5, B and C), consistent with the identification of fascin as a Rab35 effector.

Fascin is an actin cross-linking protein that organizes F-actin into tightly packed parallel bundles in protruding (filopodia) and nonprotruding (microspike) structures at the leading edges of cells (15, 16). Higher than normal fascin levels have been associated with cancer cell migration, so the protein has been proposed as a marker for cancer diagnosis and a therapeutic target (17–19). Fascin is produced in many tissues and is especially abundant in the nervous system (20). In *Drosophila*, fascin mutants (called *singed*) are female sterile and have aberrant mechanosensory bristles (21, 22) due to

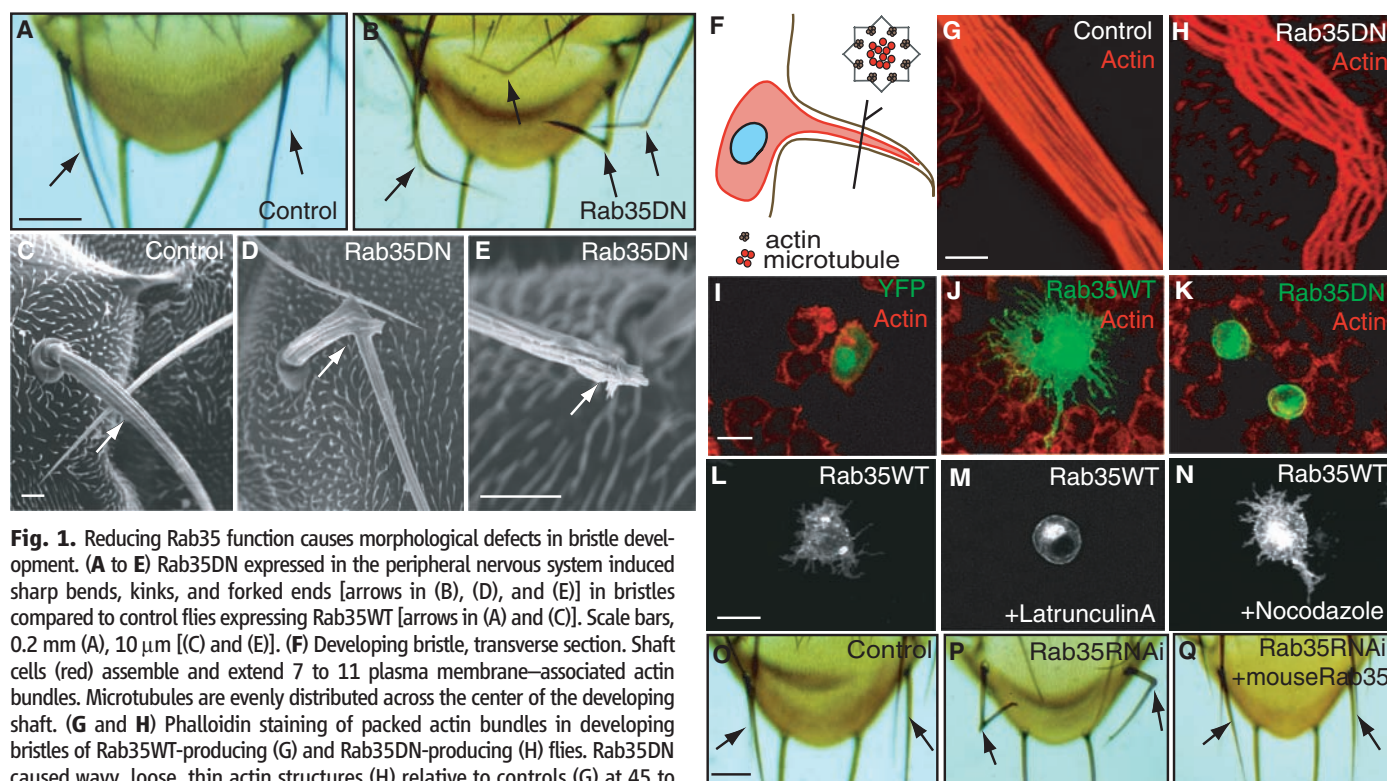


Fig. 1. Reducing Rab35 function causes morphological defects in bristle development. (A to E) Rab35DN expressed in the peripheral nervous system induced sharp bends, kinks, and forked ends [arrows in (B), (D), and (E)] in bristles compared to control flies expressing Rab35WT [arrows in (A) and (C)]. Scale bars, 0.2 mm (A), 10 μ m [(C) and (E)]. (F) Developing bristle, transverse section. Shaft cells (red) assemble and extend 7 to 11 plasma membrane-associated actin bundles. Microtubules are evenly distributed across the center of the developing shaft. (G and H) Phalloidin staining of packed actin bundles in developing bristles of Rab35WT-producing (G) and Rab35DN-producing (H) flies. Rab35DN caused wavy, loose, thin actin structures (H) relative to controls (G) at 45 to 47 hours after puparium formation. Texas Red-phalloidin staining detected the packed actin bundles. Scale bar, 10 μ m. (I to K) Relative to YFP-alone controls (I), YFP-Rab35WT (J) but not YFP-Rab35DN (K) induced filopodia-like membrane protrusions when expressed in S2 cells. Green, YFP proteins; red, phalloidin (filamentous actin). Scale bar, 5 μ m. (L to N) Latrunculin A administration completely suppressed the morphological changes caused by Rab35 (M) relative to vehicle control-treated cells (L). Treatment with nocodazole did not block the morphological changes (N). Scale bar, 5 μ m. (O to Q) Flies expressing Rab35RNAi in the peripheral nervous system had abnormal bristle morphology (P) relative to controls (O). A mouse Rab35WT transgene reversed this phenotype (Q). Scale bar, 0.2 mm.

dysfunctional actin structures. The *Drosophila* egg chamber is composed of a germline cyst surrounded by a somatic follicular epithelium. Each cyst consists of 15 nurse cells and one oocyte. Cortical cytoskeletal structures are required during late oogenesis when nurse cell cytoplasm is rapidly transferred

to the oocyte. The sterility phenotype of *singed* led us to examine the influence of Rab35DN in nurse cells (driven by tubulin-gal4 at 22°C) or follicle cells (driven by CY2-gal4). Both caused female sterility (94%). The interfering Rab35DN caused reduced ovarian actin levels relative to con-

trol flies, and ovary structure was abnormal (fig. S6, D, F, H, and J).

We tested whether the physical interaction between Rab35 and fascin was reflected in a genetic interaction. Rab35RNAi, produced in peripheral neurons, was used to damage bristle development. Altered bristle morphology was suppressed when extra fascin was supplied to the same cells (Fig. 2C). Increased fascin compensated for reduced Rab35 function, which suggests that fascin is at least one of the major proteins regulated by Rab35.

Purified GST-fascin and GST-Rab35 were mixed together or separately with purified non-muscle F-actin *in vitro*. Actin-bundling activity increased with fascin concentration (fig. S7, A and B). No effect of Rab35 on actin bundling was observed, alone or in combination with fascin (fig. S7, A and C). Thus, Rab35 has no discernible effect on actin bundling *in vitro*, but its association with fascin may be a means to control when or where actin is bundled *in vivo*.

Perhaps activated Rab35 recruits fascin to a subcellular location where fascin stimulates actin bundling. To explore this idea, we first examined the relative locations of Rab35 in different cell types and its association with fascin in mammalian cells. Rab35WT was enriched near the plasma membrane (Fig. 3, D to F, and figs. S6G and S8A)

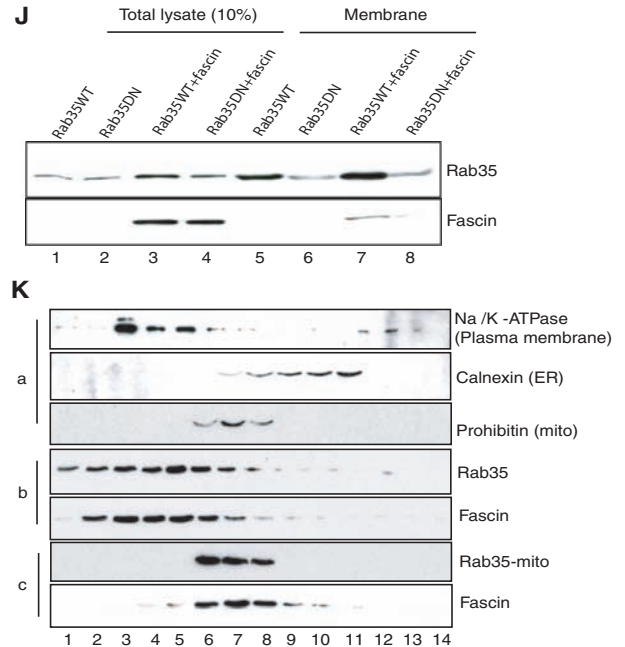
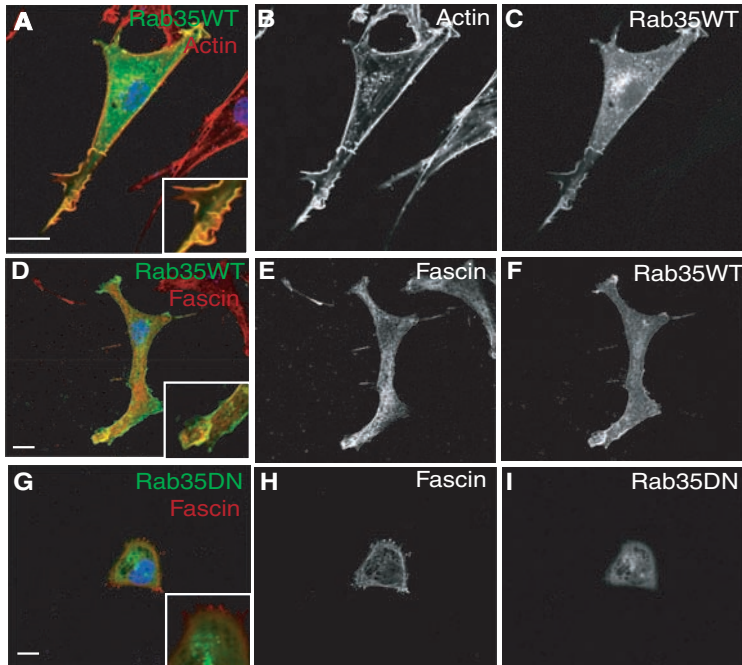
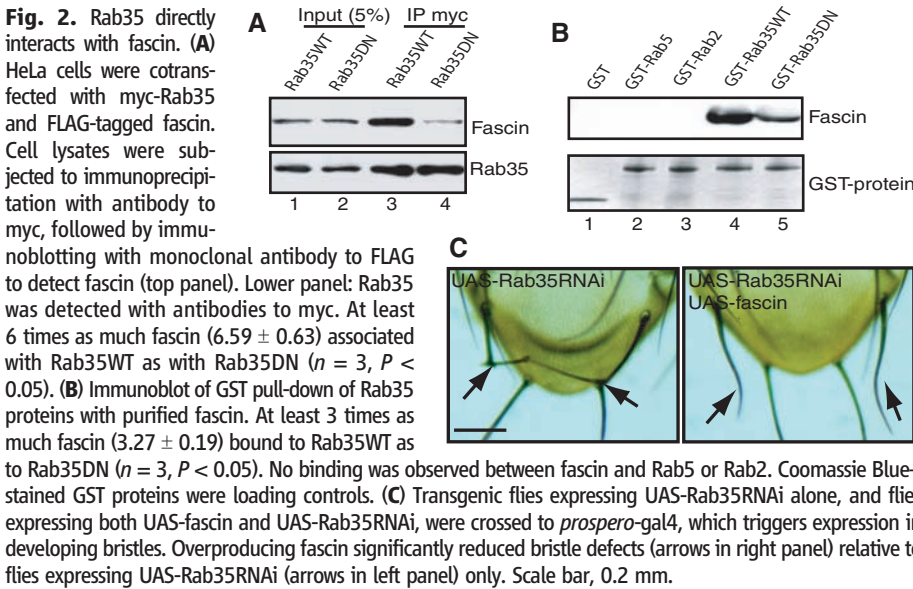


Fig. 3. Rab35 associates with fascin near the plasma membrane. **(A to C)** NIH 3T3 cells expressing YFP-Rab35 [(C) and green in (A)] were costained with actin [(B) and red in (A)] to show the colocalization of the two proteins at plasma membranes, membrane ruffles, and leading edges of cells. Scale bar, 5 μm . **(D to I)** NIH 3T3 cells producing either YFP-Rab35 WT [(F) and green in (D)] or YFP-Rab35DN [(I) and green in (G)] were costained with antibodies to fascin [(E) and (H) and red in (D) and (G)] to show the colocalization of the Rab35 and fascin proteins. Scale bars, 5 μm . Insets in (A), (D), and (G) show higher-magnification views of the edges of cells. **(J)** Rab35WT enrichment in a membrane fraction of cells that had undergone the same treatment as in (D) to (I) (lane 7, upper panel), compared to the fractionation properties of Rab35DN (lane 8, upper panel; 33.4% increase in membrane-associated Rab35 normalized to the total Rab35

level). More fascin was observed in the membrane fraction with Rab35WT (lane 7, lower panel) than with Rab35DN (lane 8, lower panel; 17.7% enrichment of membrane-associated fascin with Rab35WT normalized to the total fascin level); 10% of total protein lysates were loaded as controls (lanes 1 to 4). **(K)** Subcellular fractionation of NIH 3T3 cells. (a) Three markers were used to show the separation of different membrane compartments. (b) Cells treated as in (D) to (I) were fractionated. Rab35WT and fascin fractionated mainly with the plasma membrane marker Na⁺- and K⁺-dependent ATPase (enriched in fractions 3 to 5), but not with the endoplasmic reticulum marker calnexin or the mitochondrial marker prohibitin. (c) Cells expressing YFP-Rab35-mito were also fractionated. An enrichment of fascin in the mitochondrial fraction was observed (fractions 6 to 8). From left to right, 2.5 to 25% iodixanol gradients.

and colocalized with fascin at the leading edge of filopodia and within microspikes in lamellipodia (Fig. 3, D to F). Rab35DN caused severe alteration of cellular structure and accumulated to a greater extent in the cytosol than along the membrane (Fig. 3, G to I, and figs. S6H and S8B). In the presence of Rab35DN, less membrane-associated fascin was observed (Fig. 3, G to I). The membrane association of Rab35 and fascin was confirmed by a cell fractionation analysis; 33.4% of Rab35 fused to yellow fluorescent protein (YFP-Rab35) and 17.7% of fascin fractionated with the membrane fraction (Fig. 3J). The association of fascin with the membrane fraction was at least partially dependent on Rab35, because less Rab35 and less fascin associated with the membrane in cells where Rab35DN was expressed. Thus, Rab35 may bring fascin to the plasma membrane to influence subcortical actin structure and initiate filament bundling.

If fascin mediates the effects of Rab35, then Rab35-induced filopodia formation should be reduced when fascin function is blocked. Fascin was depleted in *Rab35*-expressing cells by introducing fascin small hairpin RNA (16). The interfering RNA significantly blocked filopodia

formation induced by Rab35 (fig. S9, B and C). Phosphorylation of fascin at Ser³⁹ is important for its actin-bundling activity and proper localization to filopodia (15, 16). We produced point mutants that mimic the active dephosphorylated (Ser³⁹ → Ala, S39A) or inactive phosphorylated (Ser³⁹ → Asp, S39D) forms of fascin (15, 16). Expression of tTomato-tagged S39A or S39D fascin mutants in NIH 3T3 cells along with Rab35 had opposite effects on filopodia formation (figs. S9, D to F, and S10, A to I). The S39A mutant in combination with Rab35WT caused more protein to accumulate at the tip of cell extensions (figs. S9E and S10, D to F) relative to wild-type fascin plus Rab35WT, but no significant increase in the number of filopodia was observed (fig. S10J). In contrast, S39D in combination with Rab35 reduced the number of filopodia (fig. S10J). In these cells most of the Rab35WT protein remained near the plasma membrane (figs. S9F and S10, G to I). These results are consistent with a role for fascin as a downstream effector of Rab35 in filopodia formation.

We constructed a gene encoding a modified form of Rab35 targeted to the outer mitochon-

drial membrane, a location that normally has modest levels of fascin or assembled actin and no detectable Rab35 (Fig. 4, A to D). When Rab35DN was used in this experiment, the modified protein was on the surface of mitochondria (Fig. 4F). No discernible change in actin structure was observed in the vicinity of mitochondria (Fig. 4H and fig. S11, C and D). In contrast, when Rab35WT was brought to the mitochondrial outer membrane (Fig. 4, I to L), the mitochondria were consistently decorated with increased actin meshworks (Fig. 4L and fig. S11, A and B). As a control, Rab35WT targeted to mitochondria in the same manner did not cause actin assembly in the vicinity of mitochondria (Fig. 4, M to P). Fascin relocation to mitochondria was confirmed by cell fractionations. Mitochondrial enrichment of fascin was observed when Rab35WT-mito was produced (Fig. 3K). Thus, relocation of Rab35 can drive the location of actin assembly.

Our results show that a Rab35 effector protein, fascin, is able to stimulate local actin bundling and thus control bristle and filopodia formation (fig. S11E). The exact ways in which such a mechanism may be used probably vary among cell and tissue types. In cultured cells, active Rab35 recruits fascin to drive actin bundling at the leading edge of cell protrusions. During *Drosophila* bristle development, Rab35 may recruit fascin and induce actin bundling to initiate the cytoplasmic extension required for bristle extension. Inadequate Rab35 function leads to bends and kinks in the bristles.

Conflicting results about Rab35 function have been obtained from different cell types and models. Rab35RNAi revealed a function in cytokinesis in *Drosophila* S2 cells (23); in HeLa cells, Rab35 also plays a role in cytokinesis (23). No cytokinesis phenotype was observed in mutants of *Caenorhabditis elegans Rab35*, but Rab35 transports yolk receptors in oocytes (24). In HeLa-CIITA, a cell line in which major histocompatibility complex (MHC) class II is expressed, Rab35 regulates a recycling pathway in a clathrin-, AP2-, and dynamin-independent manner (25). In Jurkat T cells, Rab35-mediated recycling appears to be clathrin-dependent (11). In PC12 and N1E-115 cells, activated Rab35 stimulates neurite outgrowth via a Cdc42-dependent pathway (12). *Drosophila Rab35*, like mammalian Rab35, is found near the plasma membrane, on intracellular vesicles, and in the cytosol (23) (Fig. 3, A to C). This broad distribution contrasts with more discrete locations of other Rab proteins, including many we studied (10), which suggests that Rab35 may have diverse functions.

Interfering with Rab35 in living flies showed its importance for normal bristle morphology and its function in regulating actin assembly. The powerful influence of Rab35 on the cytoskeleton can now be at least partly explained by localization of fascin and its consequent influence on actin filament bundling.

References and Notes

1. F. A. Barr, U. Gruneberg, *Cell* **131**, 847 (2007).
2. E. S. Chhabra, H. N. Higgs, *Nat. Cell Biol.* **9**, 1110 (2007).
3. M. S. Mooseker, *Cell* **35**, 11 (1983).

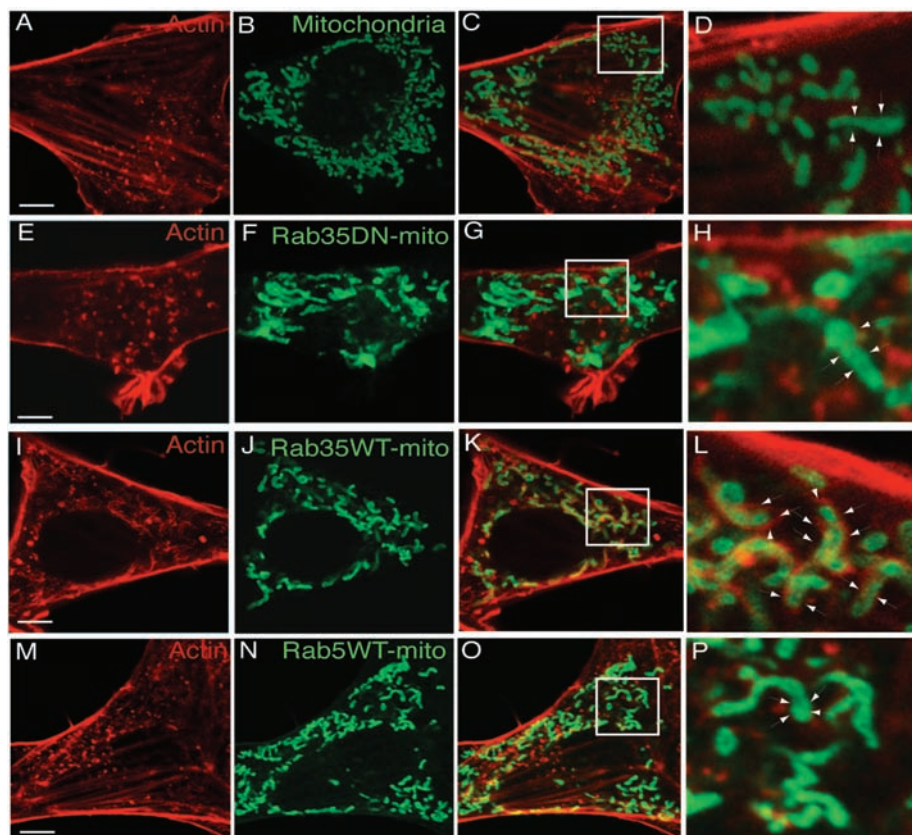


Fig. 4. Localized stimulation of actin bundling by Rab35 recruitment of fascin. (A to D) NIH 3T3 cells were stained with MitoTracker (Invitrogen; green) to show mitochondria and actin (red). Box in (C) is shown in (D) at higher magnification. Arrowheads indicate areas surrounding mitochondria. Scale bar, 5 μ m. (E to P) NIH 3T3 cells producing YFP-Rab35DN-mito, YFP-Rab35WT-mito, and YFP-Rab5-mito (all in green) were stained with phalloidin (red) to detect actin. In 20 to 30% of cells, localization of Rab35WT to mitochondria induced actin assembly in the vicinity of mitochondria (K). In parallel experiments in which Rab35DN and Rab5 were localized to mitochondria, no such enrichment of actin was observed [(G) and (O), respectively]. Boxes in (C), (G), (K), and (O) are shown in (D), (H), (L), and (P) at higher magnification. Arrowheads indicate areas surrounding mitochondria. Detectable accumulation of actin near mitochondria was observed only in (L). Scale bars, 5 μ m.

4. J. Faix, K. Rottner, *Curr. Opin. Cell Biol.* **18**, 18 (2006).
5. G. M. Guild, P. S. Connelly, L. Ruggiero, K. A. Vranich, L. G. Tilney, *J. Cell Biol.* **162**, 1069 (2003).
6. L. G. Tilney, P. Connelly, S. Smith, G. M. Guild, *J. Cell Biol.* **135**, 1291 (1996).
7. L. G. Tilney, P. S. Connelly, L. Ruggiero, K. A. Vranich, G. M. Guild, *Mol. Biol. Cell* **14**, 3953 (2003).
8. S. Pfeffer, *Biochem. Soc. Trans.* **33**, 627 (2005).
9. S. Pfeffer, D. Aivazian, *Nat. Rev. Mol. Cell Biol.* **5**, 886 (2004).
10. J. Zhang *et al.*, *Genetics* **176**, 1307 (2007).
11. G. Patino-Lopez *et al.*, *J. Biol. Chem.* **283**, 18323 (2008).
12. J. Chevallier *et al.*, *FEBS Lett.* **583**, 1096 (2009).
13. B. L. Grosshans, D. Ortiz, P. Novick, *Proc. Natl. Acad. Sci. U.S.A.* **103**, 11821 (2006).
14. S. Christoforidis, M. Zerial, *Methods Enzymol.* **329**, 120 (2001).
15. J. C. Adams *et al.*, *Mol. Biol. Cell* **10**, 4177 (1999).
16. D. Vignjevic *et al.*, *J. Cell Biol.* **174**, 863 (2006).
17. N. A. Bakshi, W. G. Finn, B. Schnitzer, R. Valdez, C. W. Ross, *Arch. Pathol. Lab. Med.* **131**, 742 (2007).
18. H. Zhang *et al.*, *J. Clin. Pathol.* **59**, 958 (2006).
19. E. Kostopoulou *et al.*, *Histol. Histopathol.* **23**, 935 (2008).
20. A. De Arcangelis, E. Georges-Labouesse, J. C. Adams, *Gene Expr. Patterns* **4**, 637 (2004).
21. L. G. Tilney, M. S. Tilney, G. M. Guild, *J. Cell Biol.* **130**, 629 (1995).
22. K. Cant, B. A. Knowles, M. S. Mooseker, L. Cooley, *J. Cell Biol.* **125**, 369 (1994).
23. I. Kouranti, M. Sachse, N. Arouche, B. Goud, A. Echard, *Curr. Biol.* **16**, 1719 (2006).
24. M. Sato *et al.*, *EMBO J.* **27**, 1183 (2008).
25. E. Walseng, O. Bakke, P. A. Roche, *J. Biol. Chem.* **283**, 14717 (2008).
26. We thank M. Fish for DNA injections; X. Huang, E. Bustamante, and C. Gauthier for help with initial experiments; Scott lab members for valuable discussion and comments; the Stanford Cell Sciences Imaging Facility

for assistance with scanning electron microscopy studies; and S. Pfeffer, A. Ghabrial, and R. Rohatgi for critical reading and comments on the manuscript. Supported by a Jane Coffin Childs Memorial Fund for Medical Research fellowship (J.Z.) and by the NIH National Technology Center for Networks and NIH Pathway grant U54 RR020843 (M.F. and M.B.). The research reported here was supported by the Howard Hughes Medical Institute. M.P.S. is an Investigator of the HHMI.

Supporting Online Material

www.sciencemag.org/cgi/content/full/325/5945/1250/DC1
Materials and Methods

Figs. S1 to S12

Table S1

References

13 April 2009; accepted 10 July 2009

10.1126/science.1174921

Regulation of Histone Acetylation in the Nucleus by Sphingosine-1-Phosphate

Nitai C. Hait,¹ Jeremy Allegood,¹ Michael Maceyka,¹ Graham M. Strub,¹ Kuzhuvilil B. Harikumar,¹ Sandeep K. Singh,¹ Cheng Luo,^{2,3} Ronen Marmorstein,² Tomasz Kordula,¹ Sheldon Milstien,⁴ Sarah Spiegel^{1*}

The pleiotropic lipid mediator sphingosine-1-phosphate (S1P) can act intracellularly independently of its cell surface receptors through unknown mechanisms. Sphingosine kinase 2 (SphK2), one of the isoenzymes that generates S1P, was associated with histone H3 and produced S1P that regulated histone acetylation. S1P specifically bound to the histone deacetylases HDAC1 and HDAC2 and inhibited their enzymatic activity, preventing the removal of acetyl groups from lysine residues within histone tails. SphK2 associated with HDAC1 and HDAC2 in repressor complexes and was selectively enriched at the promoters of the genes encoding the cyclin-dependent kinase inhibitor p21 or the transcriptional regulator c-fos, where it enhanced local histone H3 acetylation and transcription. Thus, HDACs are direct intracellular targets of S1P and link nuclear S1P to epigenetic regulation of gene expression.

Phospholipid and sphingolipid metabolites have established roles in signal transduction pathways initiated by activation of cell surface receptors. The recent identification of nuclear lipid metabolism has highlighted a new signaling paradigm for phospholipids. The best characterized of the intranuclear lipids are the inositol lipids that have critical roles in nuclear functions, such as pre-mRNA splicing, mRNA export, transcriptional regulation, and chromatin remodeling (1). Sphingomyelin has long been known to be a component of the nuclear matrix (2), but the possibility that sphingolipids are also metabolized within the nucleus has only recently emerged from observations that enzymes control-

ling sphingolipid metabolism, including neutral sphingomyelinase and ceramidase, are also present in the nucleus (3).

Sphingosine-1-phosphate (S1P) is a sphingolipid metabolite that regulates many cellular and physiological processes, including cell growth, survival, movement, angiogenesis, vascular maturation, immunity, and lymphocyte trafficking (4–6). Most of its actions are mediated by binding to a family of five heterotrimeric guanine nucleotide-binding protein (G protein)-coupled receptors, designated S1P_{1–5} (5). S1P may also function inside the cell independently of S1P receptors (4); however, direct intracellular targets of S1P have not been identified. Since the discovery that S1P is produced intracellularly by two closely related sphingosine kinase isoenzymes, SphK1 and SphK2, much has been learned about SphK1 and its functions, yet those of SphK2 remain enigmatic (7).

Because, in many cells, SphK2 is mainly localized to the nucleus or can shuttle between the cytosol and the nucleus in accordance with its nuclear localization and export signals (8), we sought to determine its function there (9). In human MCF-7 breast cancer cells, SphK2 is predominantly lo-

calized to the nucleus (10), where it is enzymatically active and can produce S1P from sphingosine (Fig. 1A). The nucleus contained high amounts of sphingosine (table S1), and SphK2 expression significantly increased nuclear abundance of S1P by sixfold and dihydro-S1P, which lacks the trans double bond at the 4 position, by twofold (Fig. 1A). Endogenous SphK2 was mainly associated with isolated chromatin and was not detected in the nucleoplasm (Fig. 1B). SphK2 was present in purified mononucleosomes fractionated by sucrose density gradient centrifugation, and its distribution paralleled that of native histones (fig. S1A). Thus, we tested whether SphK2 was associated with core histone proteins. Immunoprecipitation of proteins from nuclear extracts prepared from MCF-7 cells overexpressing SphK2 or SphK1 and subsequent Western blot analysis demonstrated that histone 3 (H3) was associated with SphK2 (Fig. 1C), but not with SphK1. H3 was also coimmunoprecipitated with catalytically inactive SphK2^{G212E} (in which glycine 212 is replaced by glutamic acid) (Fig. 1C), which does not increase nuclear S1P (4.4 ± 0.3 and 4.6 ± 0.6 pmol/mg for vector and SphK2^{G212E}, respectively); these findings suggest that enzymatic activity is not required for association of these two proteins. H3 from nuclear extracts also associated with histidine (His)-tagged SphK2 isolated with Ni²⁺-nitrilotriacetic acid (NTA)-agarose beads (fig. S1B). To further confirm the specificity of the physical interaction of SphK2 with H3, we measured in vitro association of Ni-NTA-agarose-bound His-tagged SphK2 or His-SphK1 with individually purified histones. Only H3, but not histones H4, H2B, or H2A, bound to SphK2 (fig. S1C). In contrast, none of the purified histones interacted with SphK1 (fig. S1C).

We noticed that expression of SphK2 increased acetylation of lysine 9 of H3 (H3-K9), lysine 5 of histone H4 (H4-K5), and lysine 12 of histone H2B (H2B-K12) (Fig. 2A), without affecting acetylation of other lysines or acetylation of histone H2A. In contrast, expression of catalytically inactive SphK2^{G212E} (Fig. 2A) or SphK1 did not influence acetylation of any residues examined. Although catalytically inactive SphK2^{G212E} also bound to

¹Department of Biochemistry and Molecular Biology and the Massey Cancer Center, Virginia Commonwealth University School of Medicine, Richmond, VA 23298, USA.

²The Wistar Institute and Department of Chemistry, University of Pennsylvania, Philadelphia, PA 19104, USA.

³State Key Laboratory of Drug Research, Shanghai Institute of Materia Medica, Chinese Academy of Sciences, Shanghai 201203, P. R. China. ⁴National Institute of Mental Health, National Institutes of Health, Bethesda, MD 20892, USA.

*To whom correspondence should be addressed. E-mail: sspiegel@vcu.edu